Tip-timing measurements of transient vibrations in mistuned bladed disks

Tip-timing measurements of transient vibrations in mistuned bladed disks

S. Bornassi*, G. Battiato, C.M. Firrone, T.M. Berruti

Dipartimento di Ingegneria Meccanica e Aerospaziale, Politecnico di Torino, Corso Duca degli Abruzzi, 24, 10129 Torino, Italy

Abstract

Bladed disks are usually characterized by a rich dynamic response during service due to the occurrence of several mode shapes that vibrate at resonance within the operative range. In particular, during start-ups and shutdowns, the variable speed causes a temporary crossing of resonance that cannot be neglected to determine stress envelope and safety margins of the system during its whole mission. In fact, fluid flow induces fluctuating loads with variable frequencies (non-stationary regime) on the blades being responsible of a dynamic response which does not follow the so-called steady-state (stationary) response. This paper proposes a novel post-processing method for Blade Tip-Timing (BTT) measurements for the identification of the resonance parameters of mistuned bladed disks working in non-stationary operative conditions. The method is based on a two degrees of freedom model (2-DOFs) and focuses on transient resonances in which two mistuned modes with close resonance frequencies are involved in the dynamic response. In such circumstances, the identification method based on the single degree of freedom (1-DOF) model usually fails.

To verify the effectiveness of the method, numerical and experimental investigations have been performed. First, a mathematical simulator based on a lumped parameter model of a bladed disk system is used to generate the BTT simulated data. Experimental signals are measured using a commercial BTT system through a set of optical probes mounted circumferentially around a rotating dummy blisk. It is shown that the method produces accurate predictions for the numerical simulation, even in the presence of considerable noise levels. Moreover, experimental results confirm a successful implementation of the method on the actual BTT measurements.

Keywords: Non-stationary vibration response, Linear sweep rate, Vibration parameters identification, Frequency splitting, Blade tip-timing measurements

1. Introduction

Turbomachinery rotor blades are extremely prone to vibration-induced fatigue failures, which significantly threaten the safety and integrity of the whole mechanical assembly. In fact, resonant vibration and flutter instability are the most common types of vibration problems causing High Cycle Fatigue (HCF) damages in gas turbine engines [1]. Therefore, monitoring the blade vibrations is of great importance for assessing the health of turbomachinery. In addition, the identification of the blades vibration parameters is of particular interest for the mechanical designers, since this allows to validate and update the mathematical model of the bladed disks from the early stages of the design.

Generally, detecting the vibratory response in turbomachinery is not a trival process, due to the rotating environment and harsh operating conditions. The conventional method for vibration measurement in turbomachinery consists of installing strain gauges on the blades' airfoils. However, this method is not efficient due to several reasons, such as the direct attachment of the strain gauges only to few blades, the complex and expensive installation procedure, the complicated data transmission and finite lifetime. These drawbacks severely limit the use of this technology for a cost-effective health monitoring of the turbine blades.

To overcome these difficulties, the Blade Tip-Timing (BTT) technique has been developed since the '70s as an alternative to strain gauges. Currently, BTT is recognized as the most promising non-contact technique in turbomachinery industry for the blade vibration monitoring [2–5]. This technique enables simultaneous measurement of all the blades by non-contact sensors (capacitive, optical, eddy current). With respect to the traditional strain gauge technique, BTT measured signals are inherently under sampled due to the fact that only one sample can be taken by each sensor within a single revolution. To work through this problem, different signal post-processing analysis methods have been developed. The earliest one is the well-known single parameter method proposed by Zablotsky and Korostelev [6] in 1970. The method is based on a single degree of freedom vibrating system and requires the measurements from only one sensor. The maximum vibration amplitude can be obtained by calculating the peak-to-peak value of the sensor signal during the crossing of a resonance. Heath and Imregun in [7] then modified this method by considering the effects of blade vibration for the calculation of the arrival time. Later in [8] Heath developed the two parameters plot method for the identification of the maximum resonance amplitude and the engine order (EO) of synchronous resonances by using two BTT sensors. An improvement of

*Corresponding author.
Email address: saeid.bornassi@polito.it (S. Bornassi)

the two parameters plot was proposed by Rigosi *et al.* [9], with a focus on the Engine Order (EO) and maximum vibration amplitude identification. They verified the method through a BTT experimental campaign on a rotating dummy disk using optical BTT sensors, and then compared the post-processed response with the one identified from the strain gauges analysis.

The analysis methods introduced so far deal with 1-DOF models. In the cases of more than one mode participation in the vibratory response the identification method must be customized for multiple modes. To this end, Schlagwein and Schaber [10] proposed a multi-degrees-of-freedom model for the identification of the vibration parameters of mistuned bladed disks. The proposed method was validated by means of a comparison between simulated data and tests on a small gas turbine.

Presently, among the BTT specialists, the sine fitting [11] is the most accepted method for the analysis of BTT data. It is based on the fitting of a sine wave with constant amplitude and phase on the BTT samples recorded by the sensors (at least three) during one or more revolutions and directly provides the forced response of all the blades. The vibration parameters can then be obtained by analyzing the forced response curve via a standard fitting procedure. This method is considerably different from the methods of single parameter and two parameters plot. In particular, the latter actually uses the sensor data recorded over the entire resonance region, while the sine fitting model applies to data detected during just one or few revolutions where the rotation speed can be considered constant or averaged. Following the idea developed by Heath and Imregun in [7], Liu *et al.* [12] considered the effect of the blade vibration in the evaluation of the time-of-arrival (ToA) in the traditional circumferential Fourier fitting method. To assess the feasibility of the method, a numerical simulation was performed in order to obtain the EO and the response amplitude. Meanwhile, the method accuracy was further assessed through experimental measuremnts. Carrington *et al.* [13] formulated the determinant and autoregressive methods and compared the results of the methods statistically using Monte Carlo simulations. Heller *et al.* [14] recently proposed a novel technique on the basis of the sensor waveform for the identification of asynchronous and synchronous single-harmonic and multi-harmonic blade vibration parameters.

An extension of the sine fitting for multiple frequency resonances was proposed by Russhard [15] for the identification of the individual blades tip amplitude, frequency and phase from the analysis of ToAs. Garrido and Dimitriadis [16] compared five different auto-regressive based methods to recover the correct frequencies when two blade modes are excited simultaneously by a synchronous vibration. The methods were validated on three

test cases in which simulated data was used. It was shown that most of the methods could precisely predicts the resonance frequencies, even in the presence of significant noise levels. Zielinski and Ziller [17] described a practical application of the BTT measurement and the signal analysis methods used at MTU for the treatment of compressors experimental data. Battiato *et al.* [18] proposed a novel layout for BTT optical sensors that is particularly suitable for the measurement of shrouded bladed disks. Furthermore, an original method for the identification of the operative deformed shape of bladed disks from the BTT measurements of all the blades was presented and proved. In general, measuring the out-of-plane vibrations of shrouded bladed disks is not a trivial task when using the traditional BTT layout where the sensors are mounted in the radial direction, facing the blade tip. Di Maio and Ewins [19] addressed this issue by applying a triangular wedge at the blade tip, so that the in-plane BTT measurement at the blade tip can be used to detect out-of-plane vibrations of the blades. A remarkable application of the BTT technology for a heavy duty gas turbine was employed by Bornassi *et al.* [20] for the purpose of the design verification of the rotating blades in compressor and turbine modules. In addition to the vibration parameters, the damping and amplitude of the blades were also identified to confirm the safe functionality of the machine in real operating condition.

BTT signals suffers from under-sampling, which makes difficult to identify the resonances parameters with the conventional signal processing techniques. To address this problem, Wang *et al.* [21] proposed a multiple signal classification method to extract the blade vibration frequency. It was shown that the proposed method can well treat under-sampled signals as well as to identify the resonance frequencies in multi-frequency vibration signals. However, the applicability of such method is limited for varying speed and high acceleration rates [22, 23]. To minimize the undersampling typical of BTT signals and achieve a good resolution signal, multiple sensor layouts are usually adopted in the BTT setups. However, the restriction in their installation is always a challenging task. In this regard, Cao *et al.* [24] presented a single-probe BTT method for blade health monitoring. The method focuses on the shift detection in the natural frequency of the cracked blades, which are extracted using a frequency domain analysis of the product signal of two blades' displacements. The performance of the proposed method was demonstrated both numerically and experimentally. Contamination of the BTT signals with various noise sources are unavoidable in real measurements. Wang *et al.* [25] proposed a robust sparse representation model based on the mixture of Gaussian to deal with the unknown noise in BTT measurement. Bouchain *et al.* [26] dealt with the application of a spectral analysis method based on a simple structured

sparsity model on the blade vibration spectrum. In fact, an estimation method for the analysis of sub-sampled BTT signals was proposed. The method, which was tested on simulated signals characterized by multi-frequency components, shows a good agreement with other well-established identification methods. Additionally, good achievements were obtained for a real engine test data performed on a cracked blade test case.

BTT usually needs a Once-Per-Revolution (OPR) sensor as a reference for the ToAs. In the cases where the installation of the OPR sensor is difficult, BTT methods which do not require the OPR sensor are rather welcome. To overcome this issue, Guo *et al.* [27] presented an identification method based on BTT data measured by at least three sensors. The method is based on the detection of the changing on the vibration response of a blade seen by a pairs of sensors placed next to each other. The identification of the vibration parameters of a blade can also be obtained applying the fitting displacement formula on individual BTT sensor signal. Guo *et al.* [28] further applied the same concept of the sine fitting method for the measurement of synchronous vibrations in blades. The accuracy of the proposed method was proved through experimental tests on a high speed rotor monitored by a BTT system using optical fiber sensors. In this context, Chen *et al.* [29] developed an efficient and more accurate no-OPR BTT method. Two methods based on straight line fitting and compound reference model were presented. The efficiency of the proposed methods were proved by numerical simulation, test rig implementation and a large scale turbo fan test.

The majority of the works about the vibration measurement with BTT refer to stationary operating conditions. However, when engines run with high acceleration rates, transient behavior is observed in the vibratory response. In this regard, Ayers *et al.* [30] developed a reduced order model based on the so-called Fundamental Mistuning Model for predicting the vibration response of bladed disks under high engine acceleration rates. They proposed a criteria for the critical engine acceleration rate, above which transient effects play a major role in the response. In particular, passing through a resonance with high acceleration (transient) for a tuned system has two main effects: 1) usually, it leads to a reduction of the maximum amplitude of the vibration, 2) it shifts the rotating speed at which resonance occurs. As a consequence, the steady-state response model no longer represents the actual vibration behavior of the blade during the transient resonance transition, and more realistic models should be adopted for these cases [31–33]. The identification of the vibration parameters with the classical stationary based methods leads to overestimation of damping, maximum amplitude and resonance frequency. To solve this problem, Carassale *et al.* [34] proposed an identification procedure based on the continuous wavelet transform. Recently, Bornassi *et*

al. [35] proposed a model to fit the BTT data detected during a transient resonance crossing in the presence of one isolated mode. In many BTT system, the shaft speed during each revolution is often assumed as constant for detection of the ToAs. During fast transient run up and run downs, this assumption may no longer be acceptable and can lead to an erroneous estimation of the blade tip deflection. Diamond *et al.* [36] addressed this problem by proposing an algorithm for the linear transient condition. The method application on a set of experimental data proved its higher accuracy than other conventional methods. Yue *et al.* [37] investigated the parameter identification for asynchronous vibration under a variable speed. A novel identification method based on the two sensors data interpolation was developed, and its accuracy was verified by means of a simulated model with four blades.

It is commonly accepted that the blades usually experience lower maximum amplitude under transient resonance crossings. However, this statement just holds in the case of perfectly tuned bladed disks, while higher vibration amplitudes are reported for mistuned disks operating in a transient (non-stationary) regime. In particular, it is state of the art that the maximum amplitude for a mistuned bladed disk in transient resonance sweeps can even exceed the maximum amplitude in the steady-state resonance condition [38–45]. In particular, Bohang *et al.* [41] proved the occurrence of transient amplification factor for a mistuned test case both numerically and experimentally.

This paper presents a novel post-processing analysis method for the identification of vibration parameters in a mistuned bladed disks during transient resonance crossings. Mistuning is unavoidable in the real bladed disk assembly [46, 47]. It is due to the perturbation of the cyclic symmetry characteristics of the disks, leading in most cases to the so-called frequency splitting phenomenon [48, 49]. Typical vibrating responses of tuned and mistuned (with frequency splitting) systems in stationary and non-stationary conditions are shown in Figure 1. The beating phenomenon due to transient effect is well evident in both figures. In the tuned system, the amplitude of fluctuation and the associated beating gradually decrease over time after the peak amplitude, while in the mistuned system the response is slightly different. In the mistuned system, due to the presence of two adjacent modes with two similar but different frequencies, two beating phenomena overlap giving rise to an extra modulation as visible in the red curve of Figure 1(b). A two degrees-of-freedom (2-DOFs) vibration parameters identification method for mistuned bladed disks in stationary conditions was recently presented by Bornassi *et al.* [50]. For the case of double mode resonances coming from the splitting phenomenon, they demonstrated the applicability of the method through numerical demonstrators. An analytic solution to compute the response in the cases

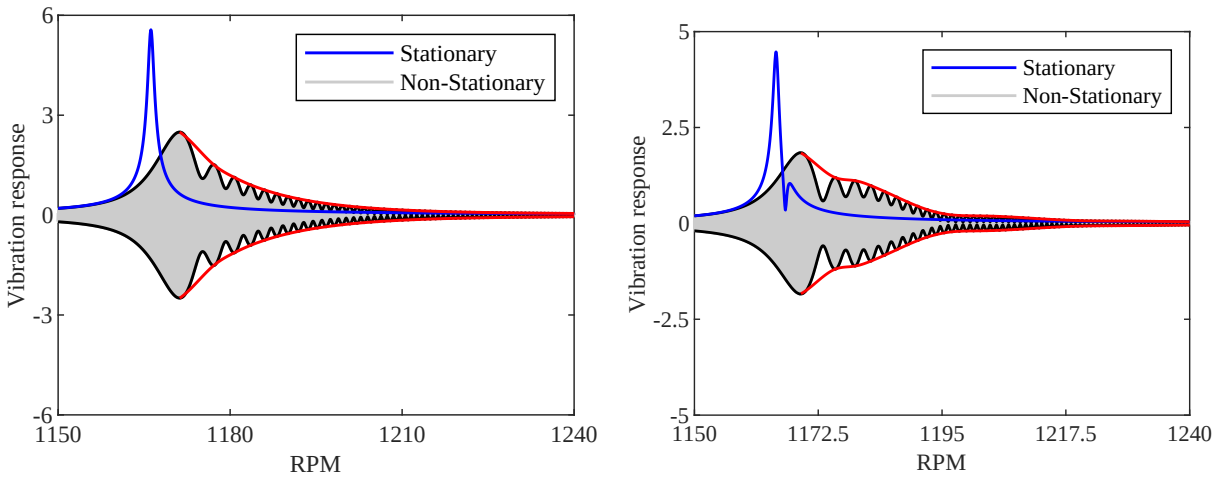

Figure 1: Comparison of the vibration response in the resonance region during stationary and non-stationary sweeps, for (a) tuned and (b) mistuned bladed disks. The grey curves are the vibratory responses of the bladed disk and the black lines show their envelopes. Red lines represent the overall behaviour of the transient envelope (for the sake of better visualization of the difference between the tuned and mistuned transient vibration response). An extra modulation of the response due to the presence of two close modes are clearly observable from the red lines associated with the mistuned case (Figure 1b). The stationary response envelopes are shown by the blue lines in order to highlight the distinction between the stationary and non-stationary cases.

where both the mistuning and transient condition was proposed by Carassale et al. [51]. They presented a solution based on a 2-DOFs system through asymptotic expansions. In case of experimental data, this kind of response, mistuned and non-stationary, will need a suitable fitting model. In this paper, it is proposed to use, as a fitting function, the one given by Markert and Seidle [33] for 1-DOF, non-stationary response under a harmonic force excitation, here extended to two degrees of freedom. This function, although approximate, has the advantage of fitting experimental data with a satisfactory convergence time. The vibration characteristics of the blades, such as the amplitude, frequency, damping, and phase, can be extracted from the 2-DOFs fitting of the recorded BTT sensor signals. The fitting analysis is performed through the nonlinear least square optimization technique.

The structure of the paper is organized as follows. In Section 2, a brief description of the BTT measurement technique is presented. Section 3 introduces the mistuning characteristics and splitting phenomenon. Section 4 presents the non-stationary vibration identification model based on a 2-DOFs vibrating system. Additionally, the BTT representation of the model and the identification algorithm are described. The performance of the proposed

method is then investigated under simulation and experimental test cases in Sections 5 and 6 respectively. The conclusions are finally summarized in Section 7.

2. Tip-Timing technique

The working principle of the BTT technique is based upon the concept of ToA. As shown in Figure 2, each non-contact sensor, mounted on the stationary casing, detects and records the ToA of the passing blade. By comparison of the ToA of the vibrating blade (recorded by the sensors) with the expected ToA for the non-vibrating blade (theoretically calculated), the time difference (lead or lag) due to vibration can be computed. This time difference is then interpreted as the blade tip displacement. The displacement data can be analyzed to determine the vibration properties of the blades: resonance peak amplitude and frequency, damping and number of waves along the hoop direction corresponding to the engine order excitation.

The procedure behind the BTT technique can be briefly described in three steps:

- Recording ToA of the vibrating blade.
- Converting ToA to the blade tip deflection.
- Extracting vibration parameters though the identification algorithms.

3. Mistuning Frequency splitting

This paper focuses on cases where the frequency response of the blade does not have a single peak at resonance, but two peaks close in frequency, as in the case of the blue curve in Figure 1(b). This phenomenon is called "frequency splitting" and it is due to the lack of a perfect cyclic symmetry in a bladed disks, i.e. mistuning [52, 53]. In fact, although the turbine bladed disks are designed to be cyclically symmetric, a slight discrepancy from the ideal design shape is unavoidable in the real turbines. Variations from blade to blade or sector to sector are typically caused by manufacturing tolerances, material imperfection and wear during machine operation. Destruction of cyclic symmetry has an effect on the forced response of the bladed disk. If the asymmetry is relatively small, a typical effect is that two orthogonal modes, related to the same nodal diameter, which in cyclic condition vibrate in resonance at the same frequency, vibrate at two different frequency values. This leads to the presence of two peaks instead of one, at the resonance in the frequency response curve.

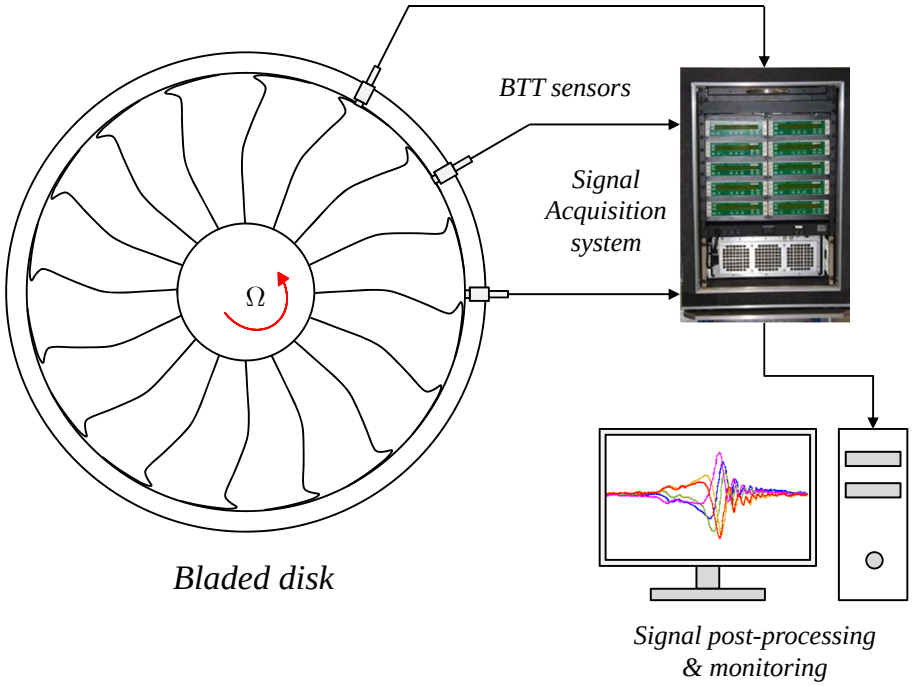

Figure 2: Schematic setup of a BTT measurement system. The non-contact sensors installed on the stationary casing so as to detect the vibration response of the blades while passing in front of them. The BTT signals are then transferred to the acquisition box for pre-processing analysis like filtering of the noises and converting the electric signals to the meaningful blade vibration signals. Finally, the deflection signal are post-processed by special under-sampled signal analysis approaches in order to extract the vibration characteristics of the blades (e.g. natural frequency, damping and amplitude).

The paper analyses the case where the resonance with a double peak is detected with a high acceleration (or deceleration) ramp. Thus the blade response is a non-stationary response as depicted in Figure 1(b).

4. Mathematical formulation

In this section, the theoretical aspects behind the proposed transient method based on the dynamics of a 2-DOFs system, as well as the fitting procedure for the identification of the blades' vibration parameters are presented.

4.1. 2-DOFs transient model

When the vibrating response of a system is dominated by only two modes, the system can be modelled as a 2-DOFs oscillator. In the case of mistuning frequency splitting, this approximation is not quite far from the actual dynamical behaviour. Whenever the two orthogonal modes are well separated from the rest of the modes in the same modal family,

i.e. when the two modes are isolated [49], the dynamic response of the bladed disk can be obtained as the superposition of these two active modes. Therefore, the two modes represent a good modal basis that well represents the bladed disk dynamics.

The equations of motion of a bladed disk in generalized coordinates η_j by considering two active modes involved in the dynamic response can be written as:

$$\ddot{\eta}_j + 2\zeta_j \omega_{n_j} \dot{\eta}_j + \omega_{n_j}^2 \eta_j = f_j(t), \quad j = 1, 2 \tag{1}$$

where ζ_j, ω_{n_j} and $f_j(t)$ denote the damping ratio, natural frequency and the generalized force corresponding to the j-th mode, respectively.

Assuming a harmonic excitation $f_j(t) = \bar{f}_j e^{i\omega t}$, the solution of Eq. 1 can be expressed as:

$$\eta_j(t) = Q_j e^{i\omega t} \tag{2}$$

where Q_j is the complex amplitude function, given by

$$Q_j = |Q_j| e^{-i\psi_j} \tag{3}$$

where Q_j and ψ_j represent respectively the magnitude and phase of the complex amplitude function.

In stationary conditions, the so-called steady-state complex amplitude is expressed as [54]:

$$Q_j = \frac{\delta_j}{\left(1 - r_j^2\right) + \left(2\zeta_j r_j\right)} \tag{4}$$

in which

$$r_j = \frac{\omega}{\omega_{n_j}} \ , \ \delta_j = \frac{\bar{f}_j}{k_j} \tag{5}$$

whit k_j representing the modal stiffness of the mode j.

In non-stationary condition, when the rotating speed changes linearly as:

$$\Omega(t) = at + \Omega_0 \tag{6}$$

Markert and Seidle [33] proposed the following approximate closed form solution for Q_j:

$$Q_j = B_j \left\{ 2e^{-v_j^2} + \frac{i}{\sqrt{\pi}} \frac{2v_j}{2v_j^2 - 1} \right\} \tag{7}$$

in which

$$B_j = \frac{1-i}{4\sqrt{1-\zeta_j^2}}\sqrt{\frac{\pi}{\alpha_j}}\,\delta_j \;\;;\;\; v_j = -\frac{1+i}{2\sqrt{\alpha_j}}\left(r_j + i\lambda_j\right) \;\;;\;\; \lambda_j = -\zeta_j + i\sqrt{1-\zeta_j^2} \;\;;\;\; \alpha_j = \frac{EO\,a}{\omega_{n_j}^2} \tag{8}$$

being a the sweep rate of the rotating speed, Ω_0 the initial rotating speed and EO the engine order of the excitation.

The response of the system can be obtained as a linear combination of the two modes, ϕ_1 and ϕ_2. Since the EO excitation corresponds to a traveling force for the bladed disk, the two modes will participate to the response according to a $\pi/2$ phase shift in time, i.e., the two modes are orthogonal in time, The response of the system can thus be expressed as:

$$x\left(t\right) = \Re\left(\phi_1\,\eta_1\left(t\right) + e^{\frac{i\pi}{2}}\,\phi_2\,\eta_2\left(t\right)\right) \tag{9}$$

4.2. BTT implementation

When a blade passes in front of a sensor located at a given angular position θ, the angular distance traveled by the blade at the k-th revolution can be obtained as:

$$\left(\omega t\right)_k = \mathrm{EO}\left(\varepsilon + \theta + 2\pi k\right) \tag{10}$$

where ε is the angular position of the blade at $t = 0$.

Substituting Eq. 10 into Eq. 2, the generalized coordinates from the sensor point of view for the k-th revolution can be rewritten as:

$$\eta_{jk} = Q_j e^{iEO(\varepsilon+\theta+2\pi k)} \tag{11}$$

After introducing $\bar{\phi}_1 = \phi_1\delta_1$ and $\bar{\phi}_2 = \phi_2\delta_2$, the blade response seen by the sensors in k-th revolution is obtained as:

$$x_k = \Re\left(\bar{\phi}_1\,\eta_{1k} + e^{\frac{i\pi}{2}}\,\bar{\phi}_2\,\eta_{2k}\right) \tag{12}$$

This equation is the main framework of the current BTT identification procedure. The unknown parameters in Eq. 12 are two natural frequencies $(\omega_{n_1}, \omega_{n2})$, two damping ratios (ζ_1, ζ_2), two modal factors $\left(\bar{\phi}_1, \bar{\phi}_2\right)$ and a phase angle $\bar{\varepsilon} = \mathrm{EO}\varepsilon$. By fitting of Eq. 12 to the BTT data collected by the sensors during the resonance, the unknown vibration parameters can be determined. Due to the nonlinear nature of Eq. 12, the curve fitting is performed through a nonlinear least square optimization technique. If EO is known, the data from

only one sensor can be used to estimate the resonance parameters. Otherwise, for unknown EO, all the sensors data are considered for the fitting. The goodness of fitting is assessed by checking the fitting residual, since the best fitting corresponds to the minimum residual. In the current work, all sensors signals are simultaneously used for the curve fitting analysis. The flow chart in Figure 3 illustrates the identification procedure. It should be noted that Eq. 7 respectively holds for the data placed at $r_j > \sqrt{1-\zeta_j^2} + \zeta_j$ for acceleration sweeps, and before $r_j < \sqrt{1-\zeta_j^2} - \zeta_j$ for deceleration sweeps [22]. This means that not all the data will be used for the fitting. For example, in the case of acceleration, the fitting procedure can be used just considering the data recorded after the rotor speed at which the corresponding steady state peak is crossed, as proved in [35].

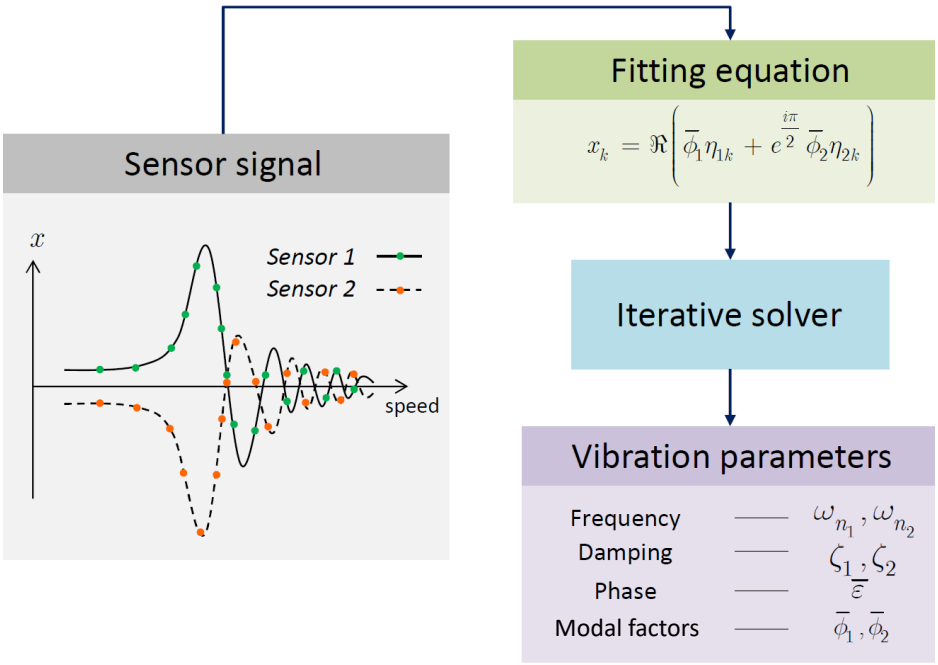

Figure 3: Flow chart represents the proposed 2-DOFs transient fitting procedure. The BTT vibration signals coming from BTT sensors are used for the vibration parameters identification through a fitting procedure. The fitting equation is given by Eq. 12. Due to nonlinear nature of this equation, the fitting process is performed by a nonlinear least square optimization technique which is an iterative approach, and the optimized vibration parameters (natural frequency, damping, amplitude and the modal factors) are extracted via this approach.

5. Numerical validation

In this section, the identification method for BTT data is first applied on a numerical model of a simple bladed disks. The validation process based on simulated data is very

common for BTT analysts, before the method is applied on experimental measurements [13, 55–57]. This is due to the advantage of testing the method performance for several combinations of resonance parameters (e.g. damping, response amplitude, amount of mistuning) through the generation of clean as well as noisy signals.

5.1. Simulated model

The proposed method is applied on simulated data obtained from a simple lumped parameter model of a bladed disk. A closed loop structure of mass-spring systems connected together is used to represent the bladed disk dynamics. Figure 4 shows the schematic layout of this model representative of a bladed disk. It can be noted that each bladed disk sector consists of two lumped masses having one DOF each. One DOF describes the motion of the blade, while the other is related to the disk. The mass and stiffness of the blade are denoted by m_b and k_b, while m_d and k_d are the mass and stiffness of the disk sector. The coupling stiffness between two neighboring sectors is indicated by k_c. As shown in Figure 4, the spring related to disk stiffness k_d is fixed to the ground.

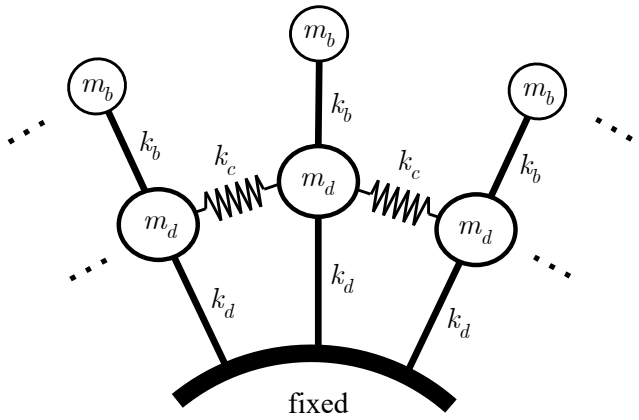

Figure 4: Lumped parameters model used for simulation. This model expresses a discrete representation of a real bladed disk assembly. It is a chain of mass-spring systems. Each sector of the bladed disks is simplified as two masses (one represents the blade mass m_b and the other one represents the disk sector mass m_d). The stiffness of the blade and the disk sector are respectively represented by two springs, k_b and k_d, and the sectors are connected through the intercoupling springs (k_c). To avoid rigid body motion, the spring associated with the disk stiffness is fixed to the ground.

The equations of motion for this system can be written as:

$$\mathbf{M}\ddot{\mathbf{q}}(t) + \mathbf{C}\dot{\mathbf{q}}(t) + \mathbf{K}\mathbf{q}(t) = \mathbf{F}(t) \tag{13}$$

where $\mathbf{q}$ is the vector of DOFs, $\mathbf{M}$, $\mathbf{C}$ and $\mathbf{K}$ are the mass, damping and stiffness matrices respectively. For further details on the structure of such matrices for mistuned cyclic symmetric structure the reader can refer to [58, 59].

The damping matrix is obtained by applying the inverse modal transformation to the modal damping matrix defined as:

$$\Phi^T \mathbf{C} \Phi = diag(2\zeta_r \omega_{n_r} m_r) \tag{14}$$

where m_r, ω_{n_r} and ζ_r are the modal mass, the natural angular frequency and the damping ratio associated to the r-th mode. Φ represents the modal matrix whose column are the eigenvectors of the undamped system.

The excitation force is applied to the blades in a traveling wave pattern. For a single EO excitation, it is defined as:

$$F_i(t) = F_0 \cos\left(\omega t - \tfrac{2\pi \mathrm{EO}}{N}(i-1)\right) \quad ; \quad i = 1, 2, 3, \ldots, N \tag{15}$$

where F_i is the force applied to the i-th blade, F_0 is the constant force amplitude and N is the number of blades.

The Runge-Kutta method is used to integrate Eq. 13 in order to find the vibratory response of the bladed disk. Then, the blades displacements at the location of the sensors can be extracted from their continuous time domain response at specific time instants, which depend on the angular position of the sensors as well as on the vibratory motion of the blades.

The bladed disk parameters in the tuned (nominal) configuration are listed in Table 1.

Table 1: Parameters of the simulated bladed disks model.

Parameter	Symbol	Value	Unit
Number of blades	N	12	
Blade mass	m_b	1	kg
Disk sector mass	m_d	4	kg
Blade stiffness	k_b	1.80e6	N/m
Disk stiffness	k_d	4.35e6	N/m
Coupling stiffness	k_c	5.00e5	N/m

Mistuning is introduced through a small variation of the nominal blade mass based on a random distribution with the standard deviation (SD) of 0.02. The blades' masses are given in Table 2.

The natural frequencies corresponding to the first modal family for the tuned and mistuned case are plotted in Figure 5. It can be noted that for each repeated mode shape,

Table 2: Mass of the blades based on a random distribution.

Blade No.	Blade mass (kg)	Blade No.	Blade mass (kg)
1	0.9940	7	1.0198
2	0.9820	8	1.0079
3	1.0127	9	1.0039
4	1.0013	10	1.0056
5	0.9963	11	1.0010
6	1.0058	12	0.9845

i.e. the modes with a number of nodal diameters (ND) larger than 0 and smaller than N/2, the splitting frequency phenomenon occurs. In particular, it is shown that for the mode with ND = 4, the repeated frequency of the tuned mode (green dot) split into two close frequencies (red stars).

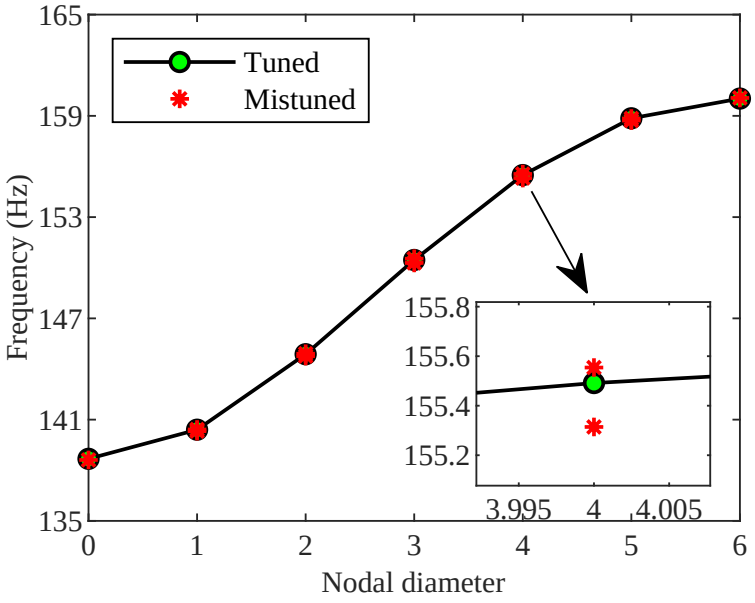

Figure 5: Diagram of natural frequencies vs the number of nodal diameters for the first modal family of the simulated lumped parameters model. The natural frequencies of the bladed disk in the tuned and mistuned configurations are computed using the mass and stiffness parameters given in Table 1 and Table 2, respectively. The green circled lines show the frequency of the tuned system and the red stars shows the frequencies of the mistuned system. Just as an example, the zoomed window displays the frequency splitting for ND=4.

5.2. Results

In this subsection the performances of the proposed method are tested on BTT signals simulated on the mistuned bladed disk. In the numerical simulations the two tuned mode shapes of the first modal family with ND = 4 are excited at resonance by a EO = 8 traveling force. The different order associated to ND and EO is due to the occurrence of aliasing. This happens because the EO = 8 traveling force is applied to 12 equally spaced blades, for this reason the traveling force is naturally under-sampled by the limited number of discrete location at which the disk is excited. The consequence is that the disk is actually excited with an EO = 4 [18]. In general, a mode shape with a certain ND can be excited by the EOs satisfying the following relationship:

$$\mathrm{EO} = z \cdot \mathrm{N} \pm \mathrm{ND}, \quad \forall\ z = 0, 1, 2, \ldots \tag{16}$$

Due to blade mass perturbation, the two mistuned modes with slightly different natural frequencies (Figure 5) replace the two tuned modes and are excited simultaneously by the EO = 8 traveling force.

The excitation frequency is varied linearly throughout each trial run. To this end, and in order to involve the transient effect into the vibrating response, the sweeping rate of the rotating speed is set to 0.10 Hz/s. The BTT simulated data are detected by two probes located at the angular positions 0° and 30°. Note that the angular position of the first probe (i.e. 0°) is arbitrarily chosen and taken as a reference for the angular location of the second probe in the direction of the disk's rotation (either clockwise or counter-clockwise).

Figure 6 shows the full vibrating response of the blade 1 with respect to the rotating speed, as well as the associated simulated BTT sensors signals. For this case, the modal damping ratios of the two active modes are assumed to be equal to 0.0005. The non-stationary effect can be clearly observed as several beats propagate in the blade response after the maximum amplitude is reached. Additionally, the contribution of the two modes appears as a second large beat in the response causing a modulation as already shown in Figure 1(b).

According to the flow chart in Figure 3, the fitting procedure is performed by Eq. 12 including all BTT sensor data. After having obtained the unknown vibration parameters from the 2-DOFs non-linear least square fitting process, the response envelope or the sensors signals can be reconstructed and compared with the exact response already computed by numerical solution of the governing equations (Eq. 13).

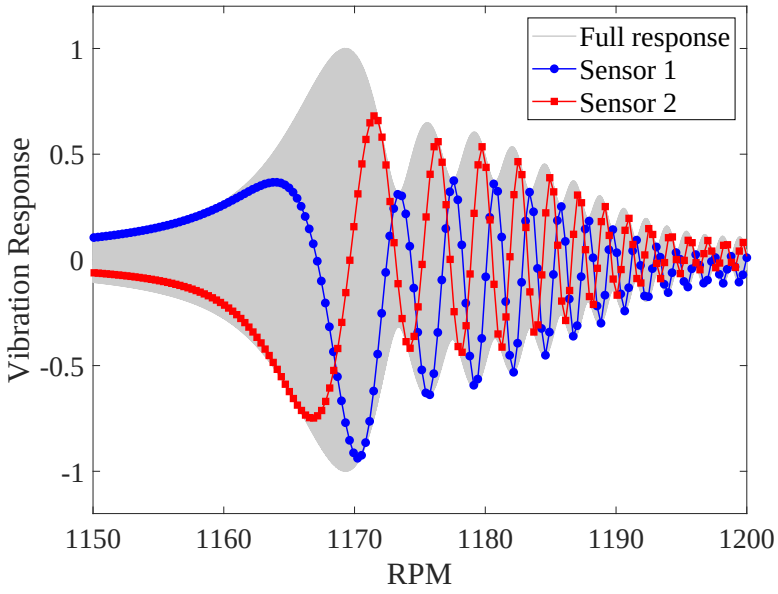

Figure 6: Vibration response and BTT sensor data associated to the mode ND = 4 excited by the EO = 8, for a rotating speed sweep rate of $0.10Hz/s$ and modal damping ratios $\zeta_1 = \zeta_2 = 0.0005$ associated to the two mistuned modes. The grey plot shows the whole vibration response of the blade, while the blue and red curves are the signals captured by the sensor 1 (0°) and sensor 2 (30°), respectively. The sensors signals are discrete while the vibration response (grey) is continuous.

Figure 7 shows the fitted displacement obtained by using the steady-state (Figure 7(a)) and transient methods in the form of response envelope (red curves).

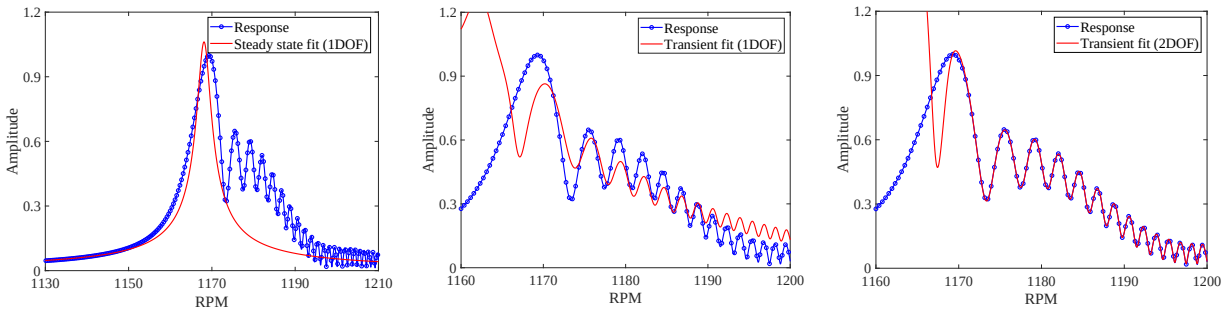

(a) (b) (c)

Figure 7: Comparison of the fitted envelopes obtained for blade 1 by three methods: steady-state (a), 1-DOF transient (b), 2-DOFs transient (c). The blue dotted lines represents the response envelope and the red lines shows the fitted curves. Modal damping ratios of $\zeta_1 = \zeta_2 = 0.0005$ associated to the two mistuned modes are considered for the generation of numerical signals. The 2-DOFs transient method provides a perfect matching with the response envelope while the 1-DOF based steady state and transient methods show poor fitting performance.

The transient fitting is performed by both 1-DOF and 2-DOFs models. For comparison purposes the steady-state method based on a 1-DOF model is also shown in this Figure. From Figure 7(c) it can be observed that the fitted curve obtained applying the presented 2-DOFs transient method (red plot) perfectly agrees with the exact response envelope (blue plot). On the contrary, the 1-DOF transient model (Figure 7(b)) does not provide a good fitting. The 2-DOFs transient model not only captures the beating shape due to the non-stationary sweeping, but also well represents the overall shape of the envelope due to the presence of two close modes: it starts increasing after the first amplitude peak and then decreases. The 1-DOF transient method is not able to reconstruct such a behavior. It only captures the beats caused by the transient effect in a gradual decreasing trend.

Moreover, the good performance of the 2-DOFs transient fitting process can be also demonstrated directly on the BTT sensor signals. Figure 8 shows the result of the fitting algorithms on the sensor signals.

It can be noted that the steady-state fit does not capture the blade's displacements detected by the sensors 1 and 2, while better fittings are provided by the transient method in the 1-DOF and 2-DOFs fashion. In particular, it is assessed once again the superior performance of the 2-DOFs transient method over the 1-DOF one: while the 2-DOFs transient method perfectly follows the displacement oscillations measured by the sensors (green dots), the 1-DOF algorithm usually over-estimates the detected displacement amplitudes.

In general, showing the results of the fitting on the reconstructed response envelope is more effective rather than directly on the sensor signals. Therefore, only the first representation will be adopted from now on.

Table 3 lists the vibration parameters identified by the three methods. As it can be observed, the transient method based on the 2-DOFs model provides excellent predictions for both natural frequencies and damping ratios associated with the two active modes.

Table 3: Comparison of the vibration parameters identified by the steady-state and transient methods for the blade 1, $\zeta_1 = \zeta_2 = 0.0005$.

Parameters	Exact value	Steady state (1-DOF)	diff (%)	Transient (1-DOF)	diff (%)	Transient (2-DOFs)	diff (%)
Frequency 1 (Hz)	155.31	155.75	0.20	155.31	0.08	155.31	0
Frequency 2 (Hz)	155.55	—	—	—	—	155.55	0
Damping ratio 1	5.00e-4	1.43e-3	186.23	3.24e-4	35.30	4.98e-4	0.36
Damping ratio 2	5.00e-4	—	—	—	—	4.94e-4	1.20

Although the 1-DOF transient model is able to predict a good estimation for the natural frequency, the damping ratio is identified with a considerable percentage of error (35%), while for the steady-state method the error further increases up to 186%.

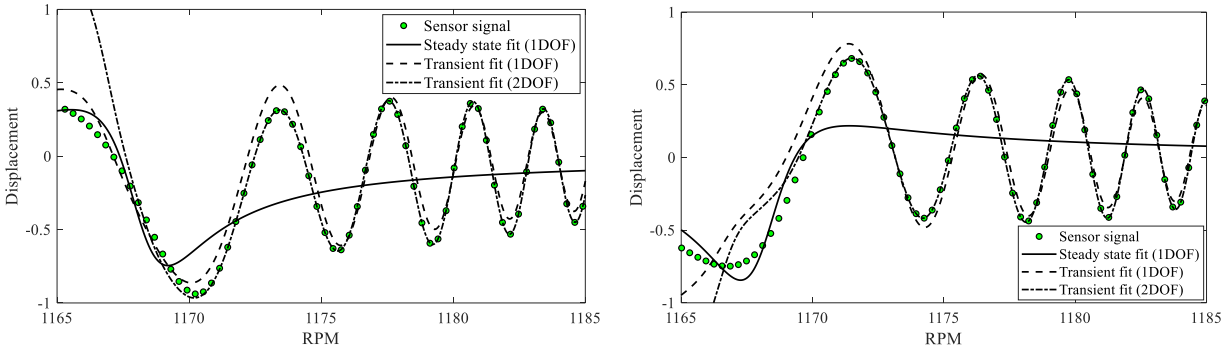

(a) (b)

Figure 8: Reconstructed sensor signal obtained by the steady-state and transient fitting methods for blade 1: sensor 1 (a) and sensor 2 (b). Modal damping ratios of $\zeta_1 = \zeta_2 = 0.0005$ associated with the two mistuned modes are considered for the generation of numerical signals. Green circles are the sensors signals, black solid lines are steady state fitting, dashed lines shows the 1-DOF transient fitting and the dash-dotted lines shows the fitting obtained by proposed 2-DOFs transient method. 2-DOFs transient method is able to fit the sensor signals significantly better than 1-DOF based steady state and transient methods.

The damping ratios of two mistuned modes are not necessarily the same in real bladed disks. Thus, a further validation is needed to check the proposed method when two different damping ratios are associated to the mistuned modes. Figure 9 shows the results of the transient fitting methods (i.e. 1-DOF and 2-DOFs) by assuming two distinct damping ratio, i.e. 0.0006 and 0.0004 for the 1-st and 2-nd mode respectively. The results confirm that even in this case the fitted curve obtained by the 2-DOFs transient model well overlaps the exact response envelope.

The values of the vibration parameters identified by the three methods are reported in Table 4.

Table 4: Comparison of the vibration parameters identified by the steady-state and transient models for blades 1 and 3, assuming the damping ratios $\zeta_1 = 0.0006$ and $\zeta_2 = 0.0004$ for the mistuned modes.

Parameters	Exact value	Steady state (1-DOF)	diff (%)	Transient (1-DOF)	diff (%)	Transient (2-DOFs)	diff (%)
				Blade 1			
Frequency 1 (Hz)	155.31	155.73	0.20	155.31	0.08	155.31	0.00
Frequency 2 (Hz)	155.55	—	—	—	—	155.55	0.00
Damping ratio 1	6.00e-4	1.53e-3	206.80	3.60e-4	28.11	5.97e-4	0.47
Damping ratio 2	4.00e-4	—	—	—	—	3.98e-4	0.55
				Blade 3			
Frequency 1 (Hz)	155.31	155.96	0.34	155.50	0.04	155.31	0.00
Frequency 2 (Hz)	155.55	—	—	—	—	155.55	0.00
Damping ratio 1	6.00e-4	1.07e-3	114.72	8.02e-4	60.38	6.03e-4	0.47
Damping ratio 2	4.00e-4	—	—	—	—	4.01e-4	0.26

The vibration frequencies and damping ratios are correctly identified by the 2-DOFs transient model (errors less that 0.5% with respect to the exact values), while the steady-state

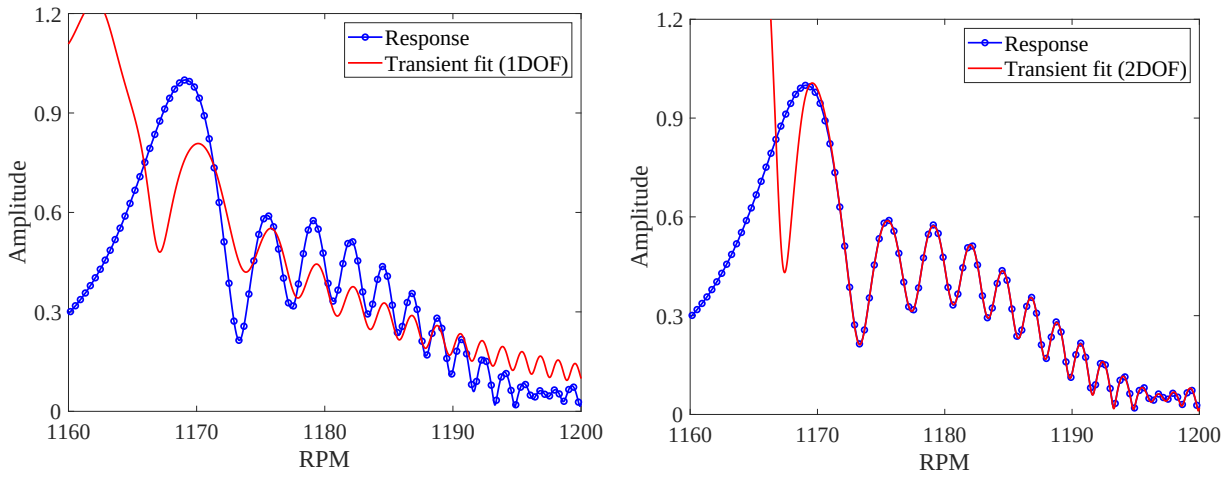

(a) (b)

Figure 9: Comparison of the fitted envelopes obtained for blade 1 by the two transient methods: 1-DOF transient method (a) and 2-DOFs transient method (b). The blue circle line represents the response envelop and the red lines show the fitted curves. Modal damping ratios of $\zeta_1 = 0.0006$ and $\zeta_2 = 0.0004$ associated with the two mistuned modes are considered for the generation of numerical signals. Again, 2-DOFs transient method is clearly better than 1-DOF transient method in fitting.

and the 1-DOF transient model cannot predict the damping ratio with a satisfactory accuracy.

In order to enhance the validation process, the study performed on blade 1 is replicated on blade 3. The results are plotted in Figure 10 and the estimated parameters are given in the second part of Table 4.

The fitted curves and the identified parameters confirm the higher precision of the 2-DOFs transient model against the 1-DOF based transient and steady-state models. Moreover, from Table 4 it can be observed that the two frequencies and the theoretical damping values (column Exact value) are the same for the two blades (blade 1 and blade 3). The disk is in fact a unique system and the two frequency values are those of the two orthogonal modes. Even though the BTT curves are different for blade 1 and blade 3, as can be seen from Figure 9 and Figure 10, the transient 2-DOFs method is robust enough to predict very similar frequency and damping values (with differences below 1%) between blade 1 and blade 3 (Transient 2-DOFs column in Table 4). The fact that, starting from two different data sets (blade 1 and blade 3) with different signal shapes, the fitting procedure identified the same parameters, as expected, confirms the goodness of the method.

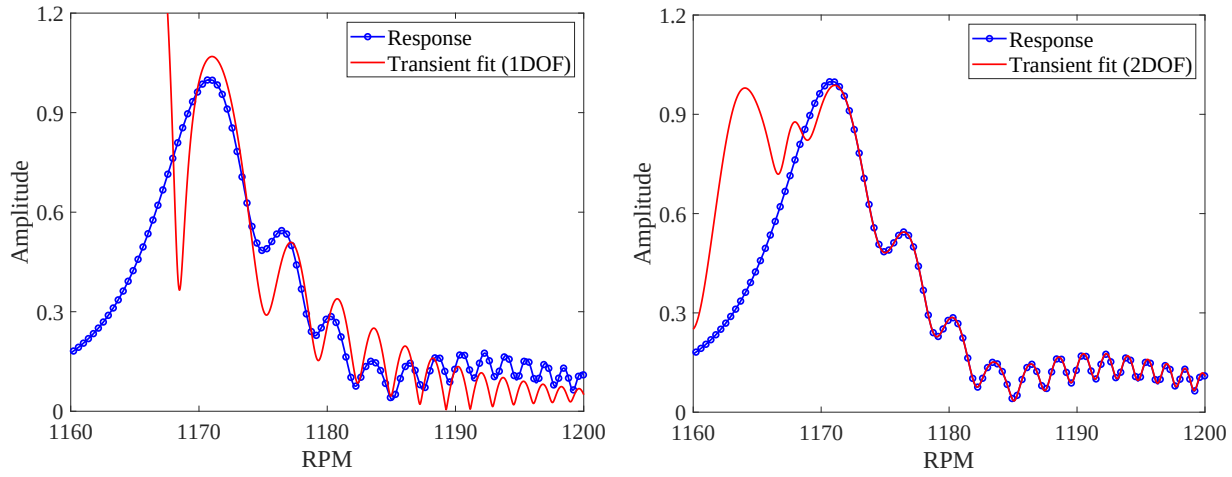

(a) (b)

Figure 10: Comparison of the fitted envelopes obtained for blade 3 by the two transient methods: 1-DOF transient method (a) and 2-DOFs transient method (b). The blue circle lines represent the response envelop and the red lines show the fitted curves. Modal damping ratios of $\zeta_1 = 0.0006$ and $\zeta_2 = 0.0004$ associated with the two mistuned modes are considered for the generation of numerical signals.

5.3. Effect of Noise

In the above case studies, the effectiveness of the proposed method was assessed for the simulated signals in the absence of noise. The real BTT signals are usually polluted by noise, which appears as a small dynamic disturbances in the BTT deflection signals [15, 60]. Although the noise is usually reduced by different filtering techniques, some sort of residual noise still affects the measured signal [61, 62]. Therefore, to evaluate the performance of the 2-DOFs transient method on a non-ideal framework, a noise study is carried out for the simulated data.

The data of two probes are contaminated by an additive white Gaussian noise. Typical noise levels [15, 60] are given in term of Signal to Noise Ratio (SNR). The noise generation is repeated 10 times for each SNR.

The mean error and the relative standard deviation across all the random trails for the damping ratios identification by the 2-DOFs transient model are plotted in Figure 11. As expected, the results confirm that the noise affects the accuracy of the fitting especially for low SNR. In fact, it is found that the smaller the SNR, the larger the percentage error in the predicted damping ratio. However, despite the noise introduction into the signals, even in the worst case (SNR = 10 dB), the errors are found to be less than 10% (i.e. actual vs predicted damping ratio).

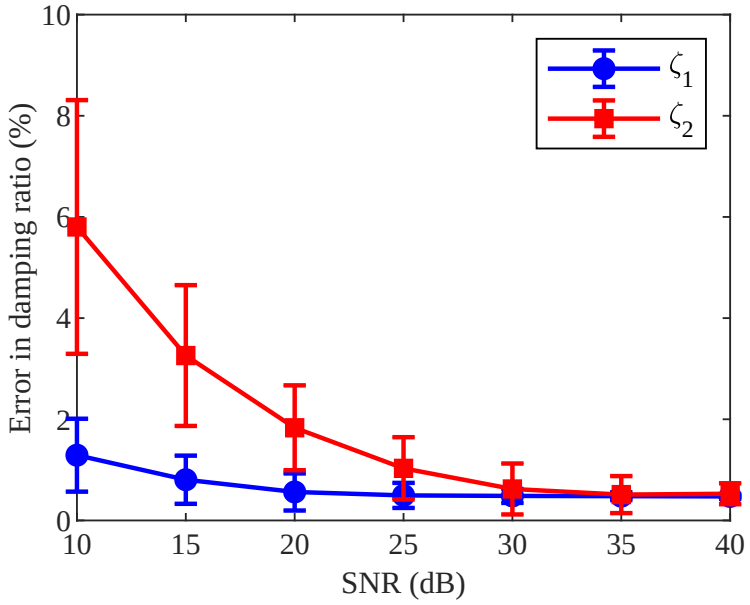

Figure 11: Effects of noise on the damping ratio estimation. Modal damping ratios of $\zeta_1 = 0.0006$, $\zeta_2 = 0.0004$ associated with the two mistuned modes are considered for the numerical signal generation. Noise randomly generated (10 times per each SNR) based on the white Gaussian noise pattern. The plot exhibits the mean value of the error and their standard deviation for 10 trials repeated for each SNR. The blue circle line shows the error for the first split mode and the red square line shows the error for the second split modes.

6. Experimental validation

To complete the validation process, an experimental campaign was organized to test the performance of the proposed 2-DOFs transient model for the identification of the vibration parameters from actual BTT measurements. The experimental results are presented and discussed in the following.

6.1. Experimental setup

As shown in Figure 12(a), the test case is an integral bladed disk (also called 'blisk') with N = 12 blades. It is made by aluminum and has a thickness of 5 mm. Each blade has a length of 150 mm, a width of 25 mm and a tip radius of 220 mm.

The rotating test rig instrumented by BTT probes is shown in Figure 12(b). The test chamber provides vacuum condition during the rotating tests. In order to excite the blade vibration, a single magnet is installed at a given axial gap from the blades. This excitation condition is such that each blade is excited by a single force pulse in one revolution, which corresponds to excite the blisk with a superposition of traveling forces having increasing EO (i.e. EO $= 0, 1, 2, \dots$). The test rig was equipped with 7 BTT optical sensors mounted on a

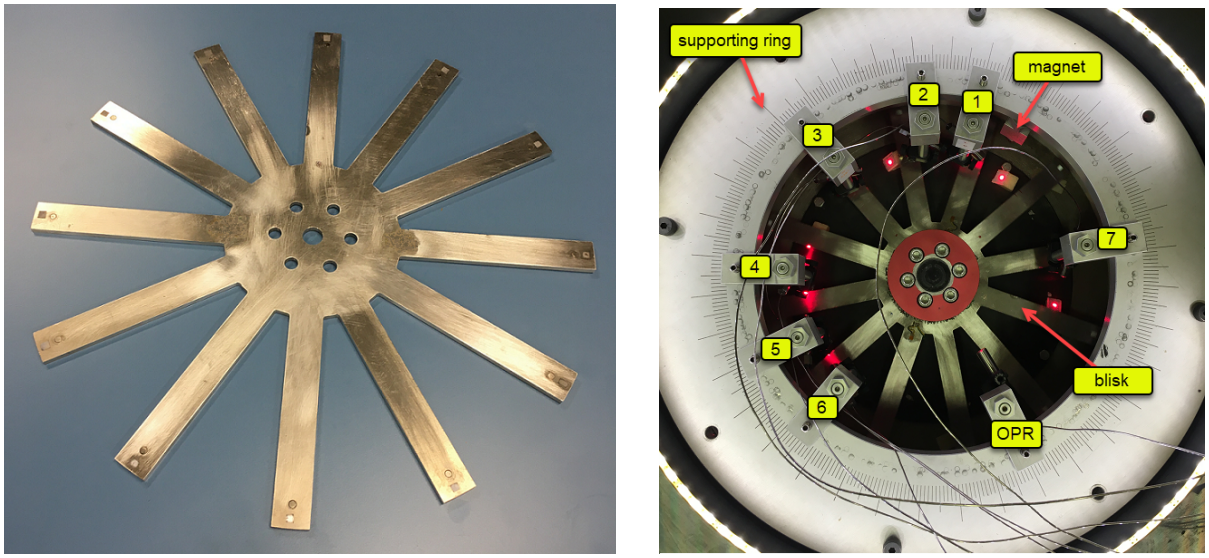

(a) (b)

Figure 12: Experimental test case and BTT setup: dummy blisk with 12 blades (a) and BTT setup illustrating the blisk at the center, sensors positioning and their numbering (b). Locations of the OPR reference sensor as well as of the permanent magnet are also shown. The sensors, OPR and magnets are installed on stationary flanges, while the test case is mounted on a rotating hub.

flange at the angular locations 0°, 22.2°, 56°, 104°, 130°, 155° and 293°. They measure the blades deflection at the radius of 162 mm. A OPR sensor was also used as a reference.

Before the dynamic tests in rotating conditions, a hammer test was performed in order to identify the blisk mode shapes and the corresponding resonance frequencies. The hammer test was carried out on the blisk with the same constrains adopted during rotation. In particular, the blisk was installed in the test rig and the hammer test performed in non-rotating conditions. A laser scanner vibrometer was used to measure the out-of-plane displacements of the blisk at the locations of the blades (one measurement point for each blade, at the same radius of the measured point by the BTT sensors), in order to identify the operative deformed shape of each mode and the corresponding number of nodal diameters. Figure 13 shows the FRF identified for one of the blade, where the peaks are associated to the resonance frequency of the first modal family in non-rotating conditions.
The resonance frequencies so obtained can be used as an initial guess for the non-linear iterative fitting process described in Section 3.

6.2. Results

Among all the excited resonances in rotating conditions, the ND = 4 mode shape was selected to test the performance of the 2-DOFs nonlinear fitting method on actual BTT

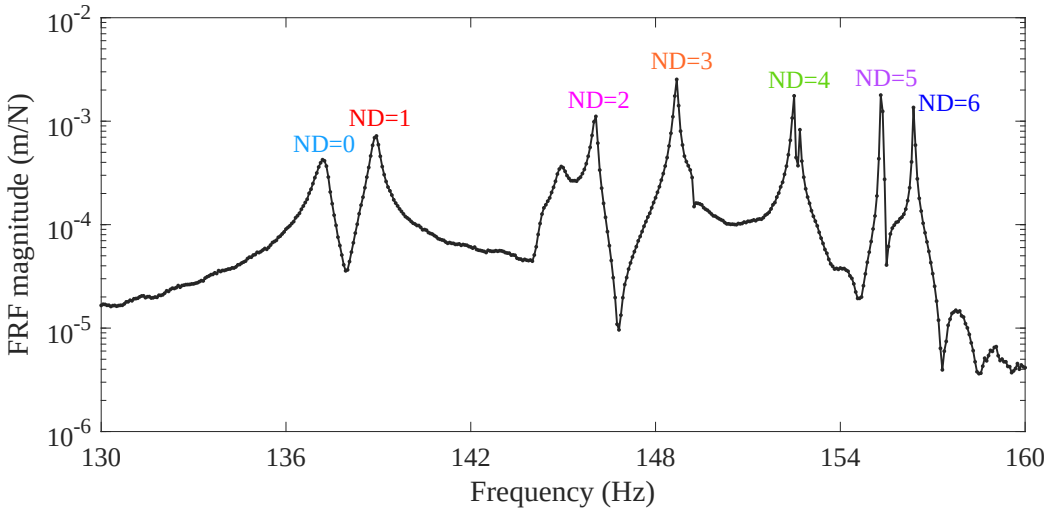

Figure 13: FRF obtained by performing hammer test on the test case. Test performed on the blisk mounted on the test rig in non-rotating condition. The blisk was excited by an hammer on the root region of the blades and a laser scanner vibrometer measured the out-of-plane vibrations of the blades. The labeled peaks are associated with the nodal diameters in the first modal family of the system, detected by the hammer test.

measurements. This choice was made for different reasons. First, from the FRF of Figure 13, the double peak associated to the selected mode confirms the presence of mistuning. Second, compared to the other mistuned mode (i.e. the mode with ND = 2), ND = 4 can be assumed to be a high number with respect to the maximum ND admissible for the blisk (i.e. ND = 6). This means that the mistuning is most likely the result of differences in the blades' geometry instead being related to the asymmetry of the disk-hub bolted connection. Third, exploiting the aliasing (Eq. 16), the ND = 4 mode shape can be excited by the traveling wave EO = 8 excitation. This ensures the resonance crossing for a rotation speed that is lower than the maximum admissible value of 3000 rpm.

The resonance frequencies of the selected modes were crossed by increasing the rotation speed linearly from 0 to 3000 rpm. The tests were carried out for two sweep rates: 0.05 Hz/s and 0.10 Hz/s, that is two different acceleration conditions. After recording the BTT signals, the fitting algorithm was implemented according to the procedure illustrated in Figure 3.

6.2.1. Sweep rate of 0.05 Hz/s

As already introduced in the numerical section, the vibration parameters of a bladed disk are evaluated by curve fitting of the BTT signals, so that either the sensors signals or the response curve can be reconstructed. In numerical simulation the response curve is already known, whereas in the experimental conditions it is an unknown curve, which has

to be identified from the measurements. For this reason, the response envelope is in this case reconstructed by the traditional sine fitting algorithm [11]. This allows to obtain the vibration amplitude at each value of the rotation speed, by fitting a sinusoidal function on the measurements of at least three sensors, for one or more rotations at the same speed. Step by step, for each speed value, the response curve visible in Figure 14 is thus constructed (blue plot).

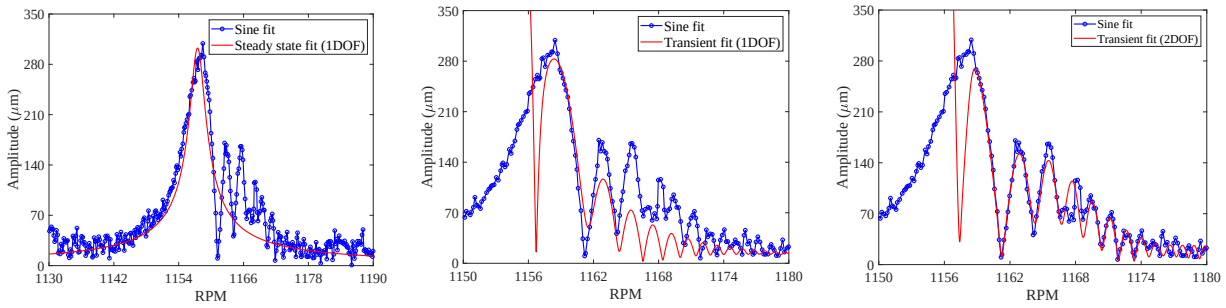

(a) (b) (c)

Figure 14: Comparison of the fitted envelopes obtained for blade 1 by three methods: 1-DOF steady-state (a), 1-DOF transient (b) and 2-DOFs transient (c), for a rotating speed sweep rate of 0.05 Hz/s. The blue dotted lines represent the response amplitude constructed by sine fitting procedure and the red lines show the fitted curves. Clearly the proposed 2-DOFs transient method shows superior fitting performance over the 1-DOF steady and transient methods.

As already done for the numerical case, the results of the fitting for the three different methods (i.e. steady-state, 1-DOF and 2-DOFs transient) can be presented either as a comparison of response curves or as a direct comparison of the sensor signals (measured and fitted).

Figure 14 compares the results of the steady-state and transient fit methods for blade 1 in terms of response envelope. Instead, Figure 15 shows the comparison in terms of sensor signals.

From the previous figures it can be clearly observed that the 2-DOFs transient method fits the response envelope and sensor signal better than its 1-DOF counterpart. The advantage of using the 2-DOFs transient method is more evident in the plots showing the reconstructed response curve (Figure 14). Furthermore, it can be observed that the typical oscillating behavior due to the closeness of the two modes natural frequencies is clearly evident in the response envelope figure. In fact, as also shown in the numerical simulations (Figure 1 and 7), a clear large beat appears modulating the maximum amplitude at a higher frequency (right after the maximum amplitude).

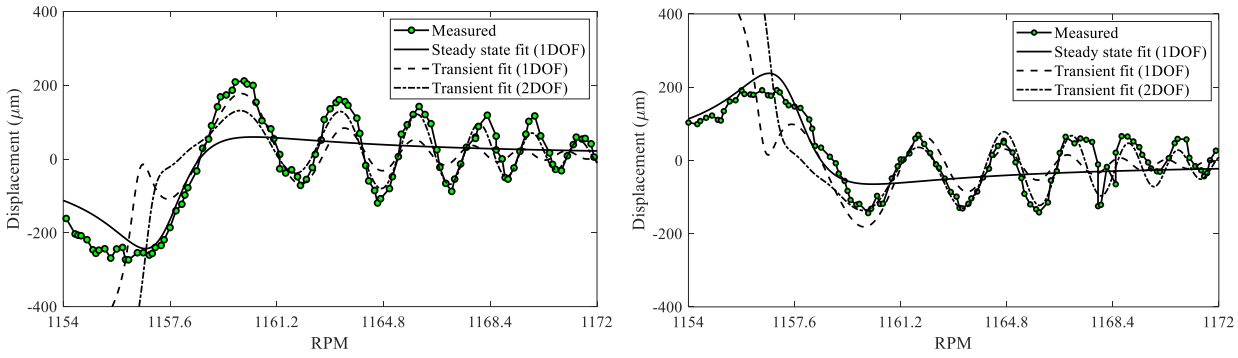

(a) (b)

Figure 15: Reconstructed sensor signal obtained by the steady-state and transient fitting models for blade 1 at the rotating speed sweep rate of 0.05 Hz/s: sensor 1 (a) and sensor 2 (b). Green circle lines are the sensors signals acquired by the BTT optical probes, black solid lines are steady state fitting, dashed lines shows the 1-DOF transient fitting and the dash-dotted lines shows the fitting obtained by proposed 2-DOFs transient method. The 2-DOFs transient method catches the transient behaviour better than the 1-DOF steady state and transient methods.

Figure 16 presents the experimental results for a different blade, blade 10. Even in this case, it must be noted that the 2-DOFs transient method performs better than the 1-DOF one.

The blade vibration frequencies and damping ratios corresponding to the two mistuned modes with ND = 4 are reported in Table 5. It can be observed that the damping value estimated by the steady-state method is completely different than the damping value obtained with the 2-DOFs transient method. Observing Table 5, the goodness of the method is confirmed by the fact that very similar frequency and damping values are found for blade 1 and blade 10, even if they are obtained from two different BTT data sets. This result is also confirmed from what was already noted in the numerical simulations, where the same vibration parameters were identified for two different blades, being the blisk a unique mechanical system.

For the experimental case described in this subsection the difference on the damping ratio obtained from the measurements of the blades 1 and 10 is at most the 10%. This value can be considered acceptable since it results from the analysis of noisy experimental data. Moreover, it must be noted that similar errors were found in the numerical simulations in the predicted modal damping ratio with respect to the assumed one (i.e. about 10% for SNR = 10 dB).

It might then be recommended to perform the measurement on more than one blade and to average the values of the obtained parameters.

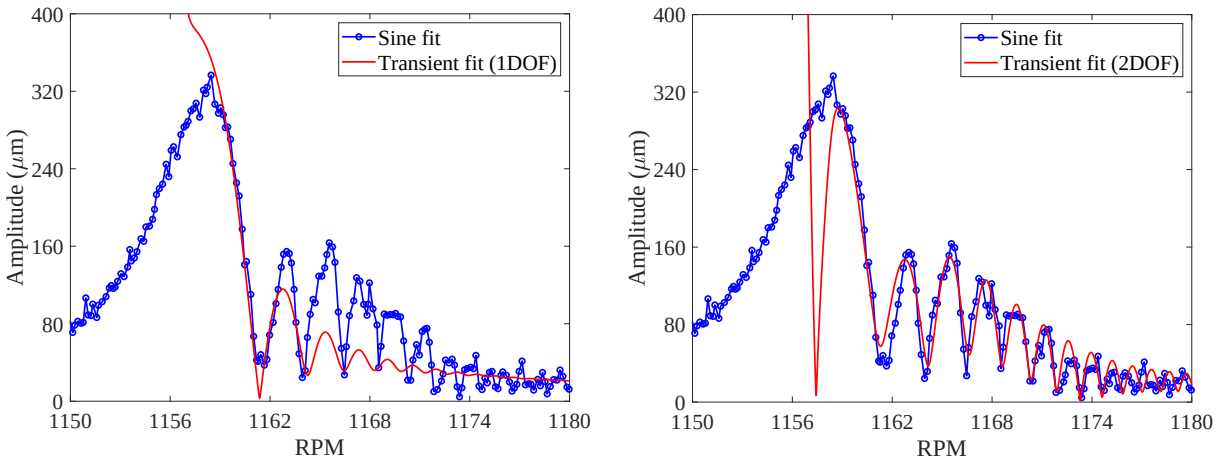

Figure 16: Comparison of the fitted envelopes for blade 10 identified by two methods: 1-DOF transient method (a) and 2-DOFs transient method (b), for a speed sweep rate of 0.05 Hz/s. The blue circle lines represent the response amplitudes constructed by sine fitting procedure and the red lines show the fitted curves. As seen, 2-DOFs transient method presents a better matching against the 1-DOF transient method.

Table 5: Comparison of the vibration parameters identified by the steady-state and transient models for blades 1 and 10 for the rotating speed sweeping rate of 0.05 Hz/s.

	Blade 1			Blade 10		
Parameters	Steady state (1-DOF)	Transient (1-DOF)	Transient (2-DOFs)	Steady state (1-DOF)	Transient (1-DOF)	Transient (2-DOFs)
Frequency 1 (Hz)	154.33	154.02	154.07	154.33	154.01	154.07
Frequency 2 (Hz)	—	—	154.26	—	—	154.25
Damping ratio 1	1.25e-3	7.16e-4	6.54e-4	1.34e-3	1.05e-3	7.31e-4
Damping ratio 2	—	—	4.10e-4	—	—	4.13e-4

6.2.2. Sweep rate of 0.10 Hz/s

In order to further assess the accuracy of the model, the tests were repeated for a higher value of rotating speed sweep rate, that is 0.10 Hz/s. The results are reported in Figure 17 for the blade 1 and 10, respectively. Table 6 quantitatively compares the identified vibration parameters. As expected, the 2-DOFs transient model still exhibits a better matching

Table 6: Comparison of the vibration parameters identified by the steady-state and transient methods for blades 1 and 10, for a speed sweep rate of 0.10 Hz/s.

	Blade 1			Blade 10		
Parameters	Steady state (1-DOF)	Transient (1-DOF)	Transient (2-DOFs)	Steady state (1-DOF)	Transient (1-DOF)	Transient (2-DOFs)
Frequency 1 (Hz)	154.53	154.04	154.06	154.53	154.02	154.06
Frequency 2 (Hz)	—	—	154.26	—	—	154.25
Damping ratio 1	1.27e-3	6.00e-4	6.98e-4	1.34e-3	7.26e-4	7.56e-4
Damping ratio 2	—	—	3.12e-4	—	—	3.27e-4

compared to the 1-DOF transient model, thus confirming the advantage of its application for the identification of transient resonances with dual mode contributions.

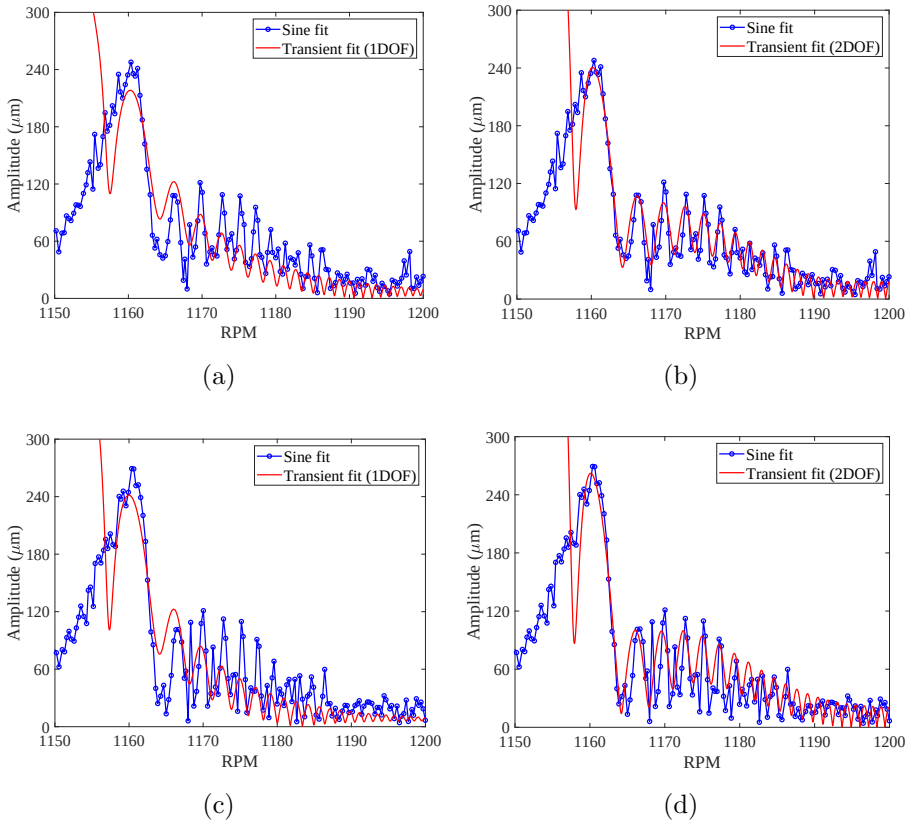

Figure 17: Comparison of the fitted envelopes for blades 1 and 10 for a rotating speed sweep rate of 0.10 Hz/s, identified by two methods: 1-DOF transient - blade 1 (a), 2-DOFs transient - blade 1 (b), 1-DOF transient - blade 10 (c), 2-DOFs transient - blade 10 (d). The blue dotted lines represent the response amplitudes constructed by sine fitting procedure and the red lines show the fitted curves. Once more, 2-DOFs transient method exhibits better performance in fitting compared to the 1-DOF method for the higher acceleration rate.

The method works well even if the data to fit are not so regular. In fact, it can be seen that the response curve to be fitted (blue curve) is not as smooth as in the case of sweep rate 0.05 Hz/s. This can be attributed to the fact that lower numbers of samples are collected in the higher acceleration rates. Despite these irregularities of the starting data, the percentage difference in damping, obtained with the measurements on blade 1 and 10 is, in the worst case, 8% (lower than in the previous sweep rate case), while no significant differences can be found for the resonance frequencies.

7. Conclusions

This paper presents a novel modal identification technique (natural frequencies, modal damping ratio, modal amplitudes) for BTT measurements of mistuned bladed disks in tran-

sient resonance crossing. The technique is based on a 2-DOFs model and can be used for a pair of mistuned isolated modes characterized by a couple of close natural frequencies.

Due to the transient crossing of the resonance region, due to fast variations of the disk rotation speed, the dynamic response of mistuned bladed disks subjected to a traveling wave EO excitation is typically characterized by two overlapping beating phenomena, which make difficult the identification of vibration parameters from the analysis of measured BTT data.

The presented technique is based on a 2-DOFs non-linear least square fitting algorithm which overcomes the limited performance of state of the art 1-DOF steady-state and transient fitting methods.

The method was numerically tested on a simulated BTT data set generated from a lumped parameter model of a mistuned bladed disk, assuming the presence of two BTT probes. It was proved that the 2-DOFs transient method could successfully predict the different natural frequencies and modal damping ratios associated to the two active mistuned modes, with errors globally less than 2%.

Furthermore, it was found that this small percentage error actually increased after the introduction of noise into the signals. As expected, the highest error on the identification of the damping ratio corresponded to the lowest SNR (i.e. percentage error was 10% for SNR = 10 dB).

The 2-DOFs transient fitting algorithm was also validated with a real BTT data set, measured on a rotating dummy bladed disk for two different acceleration rates. For both acceleration rates, the 2-DOFs model proved to fit the experimental data much better than the 1-DOF, which implies that the obtained vibration parameters are more reliable. Even in the case of higher acceleration, although the experimental data are more under-sampled and irregular, the method proved to be adequate to identify the main modal parameters of the dynamic response.

References

[1] A. Srinivasan, Flutter and resonant vibration characteristics of engine blades, in: ASME 1997 International Gas Turbine and Aeroengine Congress and Exhibition, American Society of Mechanical Engineers Digital Collection, 1997.

[2] Z. Chen, H. Sheng, Y. Xia, W. Wang, J. He, A comprehensive review on blade tip timing-based health monitoring: status and future, Mechanical Systems and Signal Processing 149 (2021) 107330.

[3] A. Abdul-Aziz, M. R. Woike, R. C. Anderson, K. Aboumerhis, Propulsion health monitoring assessed by microwave sensor performance and blade tip timing, in: Smart Structures and NDE for Energy Systems and Industry 4.0, Vol. 10973, SPIE, 2019, pp. 151–160.

[4] A. Abdul-Aziz, D. Arble, M. Woike, Data collection and analysis software development for rotor dynamics testing in spin laboratory, in: Smart Materials and Nondestructive Evaluation for Energy Systems 2017, Vol. 10171, International Society for Optics and Photonics, 2017, p. 101710L.

[5] A. Bhattacharya, V. Rajagopalan, A. Behera, R. Prabhu, N. Naithani, V. Badami, System to monitor blade health in axial flow compressors, in: 2011 IEEE Conference on Prognostics and Health Management, IEEE, 2011, pp. 1–7.

[6] I. Y. Zablotskiy, Y. A. Korostelev, Measurement of resonance vibrations of turbine blades with the elura device, Tech. rep., Foreign Technology Div Wright-Patterson AFB OH (1978).

[7] S. Heath, M. Imregun, An improved single-parameter tip-timing method for turbomachinery blade vibration measurements using optical laser probes, International Journal of Mechanical Sciences 38 (10) (1996) 1047 – 1058.

[8] S. Heath, A new technique for identifying synchronous resonances using tip-timing, Journal of Engineering for Gas Turbines and Power 122 (2) (2000) 219–225.

[9] G. Rigosi, G. Battiato, T. M. Berruti, Synchronous vibration parameters identification by tip timing measurements, Mechanics Research Communications 79 (2017) 7 – 14.

[10] G. Schlagwein, U. Schaber, Non-contact blade vibration measurement analysis using a multi-degree-of-freedom model, Proceedings of the Institution of Mechanical Engineers, Part A: Journal of Power and Energy 220 (6) (2006) 611–618.

[11] S. Heath, A study of tip-timing measurement techniques for the determination of bladed-disk vibration characteristics, Ph.D. thesis, College of Science and Technology, University of London (1997).

[12] Z. Liu, F. Duan, G. Niu, L. Ma, J. Jiang, X. Fu, An improved circumferential fourier fit (cff) method for blade tip timing measurements, Applied Sciences 10 (11) (2020) 3675.

[13] I. B. Carrington, J. R. Wright, J. Cooper, G. Dimitriadis, A comparison of blade tip timing data analysis methods, Proceedings of the Institution of Mechanical Engineers, Part G: Journal of Aerospace Engineering 215 (2001) 301 – 312.

[14] D. Heller, I. Sever, C. Schwingshackl, A method for multi-harmonic vibration analysis of turbomachinery blades using blade tip-timing and clearance sensor waveforms and optimization techniques, Mechanical Systems and Signal Processing 142 (2020) 106741.

[15] P. Russhard, Development of a blade tip timing based engine health monitoring system, The University of Manchester, 2010.

[16] J. Gallego Garrido, G. Dimitriadis, Multiple frequency analysis methods for blade tip-timing data analysis, in: Engineering Systems Design and Analysis, Vol. 4174, 2004, pp. 75–83.

[17] M. Zielinski, G. Ziller, Noncontact vibration measurements on compressor rotor blades, Measurement Science and Technology 11 (7) (2000) 847.

[18] G. Battiato, C. Firrone, T. Berruti, Forced response of rotating bladed disks: Blade tip-timing measurements, Mechanical Systems and Signal Processing 85 (2017) 912–926.

[19] D. Di Maio, D. Ewins, Experimental measurements of out-of-plane vibrations of a simple blisk design using blade tip timing and scanning ldv measurement methods, Mechanical systems and signal processing 28 (2012) 517–527.

[20] S. Bornassi, M. Ghalandari, S. F. Maghrebi, Blade synchronous vibration measurements of a new upgraded heavy duty gas turbine mgt-70 (3) by using tip-timing method, Mechanics Research Communications 104 (2020) 103484.

[21] Z. Wang, Z. Yang, S. Wu, H. Li, S. Tian, X. Chen, An improved multiple signal classification for nonuniform sampling in blade tip timing, IEEE Transactions on Instrumentation and Measurement 69 (10) (2020) 7941–7952.

[22] Z. Chen, J. Liu, C. Zhan, J. He, W. Wang, Reconstructed order analysis-based vibration monitoring under variable rotation speed by using multiple blade tip-timing sensors, Sensors 18 (10) (2018) 3235.

[23] Z. Chen, J. He, C. Zhan, Undersampled blade tip-timing vibration reconstruction under rotating speed fluctuation: uniform and nonuniform sensor configurations, Shock and Vibration 2019.

[24] J. Cao, Z. Yang, H. Li, Z. Wang, S. Tian, L. Yang, X. Chen, Single-probe blade tip timing: A novel method for anomaly identification based on frequency shift, IEEE Transactions on Instrumentation and Measurement 70 (2021) 1–16.

[25] Z.-K. Wang, Z.-B. Yang, H.-Q. Li, S.-M. Wu, S.-H. Tian, X.-F. Chen, Robust sparse representation model for blade tip timing, Journal of Sound and Vibration 500 (2021) 116028.

[26] A. Bouchain, J. Picheral, E. Lahalle, G. Chardon, A. Vercoutter, A. Talon, Blade vibration study by spectral analysis of tip-timing signals with omp algorithm, Mechanical Systems and Signal Processing 130 (2019) 108–121.

[27] H. Guo, F. Duan, J. Zhang, Blade resonance parameter identification based on tip-timing method without the once-per revolution sensor, Mechanical Systems and Signal Processing 66-67 (2016) 625 – 639.

[28] H. Guo, F. Duan, M. Wang, Blade synchronous vibration measurement based on tip-timing at constant rotating speed without once-per-revolution sensor, in: Seventh International Symposium on Precision Mechanical Measurements, Vol. 9903, International Society for Optics and Photonics, 2016, p. 990311.

[29] K. Chen, W. Wang, X. Zhang, Y. Zhang, New step to improve the accuracy of blade tip timing method without once per revolution, Mechanical Systems and Signal Processing 134 (2019) 106321.

[30] J. P. Ayers, D. M. Feiner, J. H. Griffin, A Reduced-Order Model for Transient Analysis of Bladed Disk Forced Response, Journal of Turbomachinery 128 (3) (2005) 466–473.

[31] F. M. Lewis, Vibration during acceleration through a critical speed, Trans. Am. Soc. Mech. Eng. 54 (1932) 253.

[32] R. Fearn, K. Millsaps, Constant acceleration of an undamped simple vibrator through resonance, The Aeronautical Journal 71 (680) (1967) 567–569.

[33] R. Markert, M. Seidler, Analytically based estimation of the maximum amplitude during passage through resonance, International Journal of Solids and Structures 38 (10-13) (2001) 1975–1992.

[34] L. Carassale, M. Marrè-Brunenghi, S. Patrone, Wavelet-based identification of rotor blades in passage-through-resonance tests, Mechanical Systems and Signal Processing 98 (2018) 124–138.

[35] S. Bornassi, T. Berruti, C. Firrone, G. Battiato, Vibration parameters identification of turbomachinery rotor blades under transient condition using blade tip-timing measurements, Measurement 183 (2021) 109861.

[36] D. Diamond, P. S. Heyns, A. Oberholster, Improved blade tip timing measurements during transient conditions using a state space model, Mechanical Systems and Signal Processing 122 (2019) 555–579.

[37] L. Yue, H. Liu, C. Zang, D. Wang, W. Hu, L. Wang, The parameter identification method of blade asynchronous vibration under sweep speed excitation, in: Journal of Physics: Conference Series, Vol. 744, IOP Publishing, 2016, p. 012051.

[38] A. Hartung, A numerical approach for the resonance passage computation, in: Turbo Expo: Power for Land, Sea, and Air, Vol. 44014, 2010, pp. 723–728.

[39] M. Bonhage, L. Panning-von Scheidt, J. Wallaschek, C. Richter, Transient resonance passage with respect to friction, in: Turbo Expo: Power for Land, Sea, and Air, Vol. 44731, American Society of Mechanical Engineers, 2012, pp. 1227–1237.

[40] M. Bonhage, O. P. Hentschel, L. Panning-v. Scheidt, J. Wallaschek, Transient amplification of maximum vibration amplitudes, PAMM 15 (1) (2015) 47–48.

[41] M. Bonhage, J. T. Adler, C. Kolhoff, O. Hentschel, K.-D. Schlesier, L. Panning-von Scheidt, J. Wallaschek, Transient amplitude amplification of mistuned structures: An experimental validation, Journal of Sound and Vibration 436 (2018) 236–252.

[42] Y. Kaneko, Study on transient vibration of mistuned bladed disk passing through resonance, in: Turbo Expo: Power for Land, Sea, and Air, Vol. 55270, American Society of Mechanical Engineers, 2013, p. V07BT31A002.

[43] B. Lübbe, C. Siewert, Optimization of the vibration behavior at speed-synchronous resonance of a large turbine blade during speed-up and coast-down under consideration of mistuning, in: Turbo Expo: Power for Land, Sea, and Air, Vol. 50954, American Society of Mechanical Engineers, 2017, p. V008T29A013.

[44] J. Tong, C. Zang, E. Petrov, High fidelity transient forced response analysis of mistuned bladed disks under complex excitation and variable rotation speeds, in: Turbo Expo: Power for Land, Sea, and Air, Vol. 84232, American Society of Mechanical Engineers, 2020, p. V011T30A023.

[45] T. Nakajima, K. Segawa, H. Kitahara, A. Seo, Y. Yamashita, T. Kudo, Experimental investigation of the grouped blade vibration for steam turbine by non-contact sensors, in: Turbo Expo: Power for Land, Sea, and Air, Vol. 50954, American Society of Mechanical Engineers, 2017, p. V008T29A025.

[46] S. Bornassi, H. Navazi, H. Haddadpour, Aeroelastic instability analysis of a turbomachinery cascade with magnetorheological elastomer based adaptive blades, Thin-Walled Structures 130 (2018) 71–84.

[47] S. Bornassi, H. Navazi, H. Haddadpour, Coupled bending-torsion flutter investigation of mre tapered sandwich blades in a turbomachinery cascade, Thin-Walled Structures 152 (2020) 106765.

[48] J. A. Kenyon, J. Griffin, Experimental demonstration of maximum mistuned bladed disk forced response, in: Turbo Expo: Power for Land, Sea, and Air, Vol. 36878, 2003, pp. 195–205.

[49] C. Martel, R. Corral, Asymptotic description of maximum mistuning amplification of bladed disk forced response, Journal of Engineering for Gas Turbines and Power 131 (2) (2009).

[50] S. Bornassi, C. M. Firrone, T. M. Berruti, Vibration parameters estimation by blade tip-timing in

mistuned bladed disks in presence of close resonances, Applied Sciences 10 (17) (2020) 5930.

[51] L. Carassale, V. Denoël, C. Martel, L. Panning-von Scheidt, Key features of the transient amplification of mistuned systems, Journal of Engineering for Gas Turbines and Power 143 (3) (2001).

[52] M. Nikolic, New insights into the blade mistuning problem, Ph.D. thesis, University of London (2007).

[53] Y. J. Chan, Variability of blade vibration in mistuned bladed discs, Ph.D. thesis, Imperial College London (University of London) (2009).

[54] S. S. Rao, Vibration of continuous systems, Vol. 464, Wiley Online Library, 2007.

[55] G. Dimitriadis, I. B. Carrington, J. R. Wright, J. E. Cooper, Blade-tip timing measurement of synchronous vibrations of rotating bladed assemblies, Mechanical Systems and Signal Processing 16 (4) (2002) 599–622.

[56] M. E. Mohamed, P. Bonello, P. Russhard, An experimentally validated modal model simulator for the assessment of different blade tip timing algorithms, Mechanical Systems and Signal Processing 136 (2020) 106484.

[57] L. Piechowski, R. Rzadkowsk, P. Troka, P. Piechowski, L. Kubitz, R. Szczepanik, Tip-timing steam turbine rotor blade simulator, Journal of Vibration Engineering & Technologies 6 (4) (2018) 317–323.

[58] S.-Y. Lee, M. Castanier, C. Pierre, Assessment of probabilistic methods for mistuned bladed disk vibration, in: 46th AIAA/ASME/ASCE/AHS/ASC Structures, Structural Dynamics and Materials Conference, 2005, p. 1990.

[59] T. Zhao, H. Yuan, W. Yang, H. Sun, Genetic particle swarm parallel algorithm analysis of optimization arrangement on mistuned blades, Engineering Optimization 49 (12) (2017) 2095–2116.

[60] S. Wu, X. Chen, P. Russhard, R. Yan, S. Tian, S. Wang, Z. Zhao, Blade tip timing: From raw data to parameters identification, in: 2019 IEEE International Instrumentation and Measurement Technology Conference (I2MTC), IEEE, 2019, pp. 1–5.

[61] O. Jousselin, Development of Blade Tip Timing Techniques in Turbo Machinery, The University of Manchester (United Kingdom), 2013.

[62] A. Vercoutter, M. Berthillier, A. Talon, B. Burgardt, J. Lardies, Estimation of turbomachinery blade vibrations from tip-timing data, in: 10th International Conference on Vibrations in Rotating Machinery, London, Sept, 2012, pp. 11–13.